Applied Mathematics and Computation 203 (2008) 854–863

Contents lists available at ScienceDirect

Applied Mathematics and Computation

journal homepage: www.elsevier.com/locate/amc

Homotopy analysis method for limit cycle flutter of airfoils

Y.M. Chen, J.K. Liu *

Department of Mechanics, Zhongshan University, Guangzhou 510275, China

ARTICLE INFO

Keywords:
Homotopy analysis method
Nonlinear flutter
Limit cycle

ABSTRACT

An analytical approximate method for non-linear problems, namely the homotopy analysis method, is for the first time employed to propose a new approach for the flutter system of a two-dimensional airfoil with a cubic structural nonlinearity. The frequencies and amplitudes of limit cycle flutters are described as Maclaurin series of an embedding parameter. A series of algebraic equations in the priori unknown coefficients of the series are derived. All the equations are linear except the first one. This provides us with a simple iteration scheme to seek the solutions to any desired accuracy. Numerical examples are presented to illustrate the validity and efficiency of the proposed approach. The approximations of the frequencies and amplitudes of the limit cycles are obtained very accurately. Furthermore, it is proved the frequencies are independent of the coefficient of the cubic nonlinearity, while the amplitudes are in inverse proportion to the square root of the coefficient.

1. Introduction

Homotopy, as a fundamental part of topology, has a relevant place in constructing algorithms for solving systems of algebraic equations, which is referred to as the homotoy method [1]. This method has become much more efficient and powerful since the probability-one homotopies were proposed by Chow et al. [2], and hence was widely applied and improved to solve many problems such as nonlinear systems (e.g., analog circuit simulation [3]), polynomial systems (e.g., reconfigurable space truss [4]) and nonlinear constrained optimization [5], etc. More details of its development and application in computational science can be found in Ref. [6].

In recent years, a growing interest towards the application of the homotopy technique in nonlinear problems has been devoted by the engineering practice. The main reason consists in the fact that homotopy method is to continuously deform a simple problem easy to solve into the difficult problem under study. Liao [7–10] initiated the homotopy analysis method (HAM) which does not require small/large parameters and thus can be applied to solve nonlinear problems without small or large parameters. Its main procedure is to construct a class of homotopy in a very general form by introducing an auxiliary parameter. This parameter can provide us with a convenient way to control the convergence of approximation series and adjust convergence regions when necessary. The systematical description of this method was given in Ref. [11], where the author also discussed the convergence of the approximation series and showed that, as long as the series given by HAM converges, it must converge to one solution of the studied problem. By now, the HAM has been widely used in various nonlinear problems [12–16]. Another method called the homotopy perturbation method was proposed by He [17–20] by combining the homotopy technique with the classical perturbation technique. This method also has many applications in a wide range of nonlinear problems [21].

Airfoil flutter is one of the typical self-excited systems. By extracting energy from the air, the airfoil can continue vibrating stably or unstably, which is called benign flutter or disaster flutter, respectively. The harmonic balance (HB) method is

* Corresponding author.
E-mail address: jikeliu@hotmail.com (J.K. Liu).

0096-3003/$ - see front matter © 2008 Elsevier Inc. All rights reserved.
doi:10.1016/j.amc.2008.05.095

widely used for nonlinear airfoil flutter [22]. The HB method with one dominant harmonic, i.e. HB1, is also called as the describing function method in nonlinear vibration theory. Linearized flutter systems can be obtained from the nonlinear ones by HB1 method, and then the traditional methods for linear flutters can be employed [23,24]. Equivalent linearization method is another version of the HB1 method. Liu and Zhao [25] studied the bifurcations in the oscillations of an airfoil with a cubic pitching non-linearity, and showed that results obtained by equivalent linearization method are in good agreement with numerical solutions. Shahrzad and Mahzoon [26] used the method proposed in Ref. [25] to investigate three flutter models of a two-dimensional wing, i.e., the steady linear, steady non-linear and unsteady nonlinear models. Yang [27] combined the KBM and equivalent linearization method to study the limit cycle flutter of a two-dimensional wing and a delta wing with external stores.

Liu and Dowell [28] studied the aeroelastic problems of an airfoil with a freeplay control surface by HB method. The high dimensional HB method was extensively studied in recent years [29]. It was successfully employed to investigate the aeroelastic motions of an airfoil [30]. Additionally, Cai et al. [31] used the incremental harmonic balance (IHB) method to study the limit cycle flutter of an airfoil with multiple strong nonlinearities.

The approximate solutions obtained by HB1 method are relatively accurate for low flow speeds. However, the errors of the approximate solutions become larger and larger as the flow speeds increase [23–27]. In some nonlinear flutter cases, the HB1 method may cease to be valid. In principle, the high dimensional HB method and IHB can provide approximate solutions to any desired accuracy. However, they are both relatively difficult to implement. So it is necessary to develop new easier-to-use methods which can guarantee accuracy for high flow speed and in any flutter cases. The HAM is therefore employed to propose a new approach for nonlinear flutter systems in the present paper. This approach provides us with a very simple iteration algorithm and can be used to obtain the approximations with any degree of accuracy in any flutter conditions, e.g., both weakly and strongly nonlinear flutter.

2. Equations of motion

The flutter model of a two-dimensional airfoil in unsteady flow is inherently infinite dimensional. Lee et al. [32] reduced it as a system of eight first order ordinary differential equations (ODEs). Coller and Chamara [33] derived a lower order flutter model with only six first order ODEs, which is equivalent to the one proposed in Ref. [32]. Hall et al. [34,35] proposed an orthogonal decomposition technique for transonic unsteady flows. In this paper, to introduce the proposed method briefly, we only consider the steady flow model [25–27,31].

The physical model given in Fig. 1 is a two-dimensional airfoil, oscillating in pitch and plunge, which has been employed by many authors. The pitch angle about the elastic axis is denoted by α, positive with the nose up; the plunge deflection is denoted by $\bar{h}$, positive in the downward direction. The elastic axis is located at a distance $a_h b$ from the mid-chord, while the mass center is located at a distance $x_\alpha b$ from the elastic axis. Both distances are positive when measured towards the trailing edge of the airfoil. Let $r_\alpha b$ be the radius of gyration of the airfoil with respect to the elastic axis, and ω_ξ, ω_α be the eigenfrequencies of the constrained one-degree-of-freedom system associated with the linear plunging and the pitching springs, respectively. c_α and c_ξ are the coefficients of damping in pitch and plunge respectively.

In terms of non-dimensional time $t = \omega_\alpha t_1$ (t_1 is the real time) and non-dimensional plunge displacement $\xi = \bar{h}/b$, the coupled motions of the airfoil in incompressible steady flow can be described as [25]

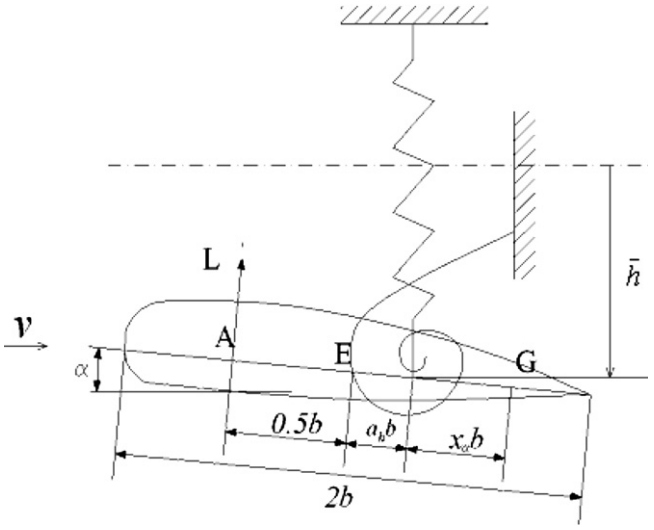

Fig. 1. Sketch of a two-dimensional airfoil.

$$\begin{cases} \mu\ddot{\xi} + \mu x_\alpha \ddot{\alpha} + \frac{c_\xi}{\pi\rho b^2 \omega_\alpha}\dot{\xi} + \mu\left(\frac{\omega_\xi}{\omega_\alpha}\right)^2 \frac{\partial V}{\partial \xi} = -2(\frac{v}{b\omega_\alpha})^2\alpha, \\ \mu x_\alpha \ddot{\xi} + \mu r_\alpha^2 \ddot{\alpha} + \frac{c_\alpha}{\pi\rho b^2 \omega_\alpha}\dot{\alpha} + \mu r_\alpha^2 \alpha \frac{\partial V}{\partial \alpha} = (1 + 2a_h)\left(\frac{v}{b\omega_\alpha}\right)^2 \alpha, \end{cases} \tag{1}$$

where the superscript denotes the differentiation with respect to t. The symbol V above represents the potential for the elastic restoring forces and in this study is given by

$$V = \frac{1}{2}\xi^2 + \frac{1}{2}\alpha^2 + \frac{1}{4}\delta_3\alpha^4, \tag{2}$$

where δ_3 is a constant. Thus, we consider pitch spring with cubic nonlinearity. Introducing the values of the parameters adopted by Liu and Zhao [25]: $\mu = 20$, $a_h = -0.1$, $b = 1m$, $x_\alpha = 0.25$, $r_\alpha^2 = 0.5$, $(\frac{\omega_\xi}{\omega_\alpha})^2 = 0.2$, $\omega_\alpha = 62.8Hz$ and the damping terms $0.1\dot{\xi}$, $0.1\dot{\alpha}$, then Eq. (1) is rewritten as

$$\begin{aligned} &0.5\ddot{\xi} + 0.25\ddot{\alpha} + 0.1\dot{\xi} + 0.2\xi + 0.1Q\alpha = 0, \\ &0.25\ddot{\xi} + 0.5\ddot{\alpha} + 0.1\dot{\alpha} - 0.04Q\alpha + f(\alpha) = 0, \end{aligned} \tag{3}$$

where $Q = \left(\frac{v}{b\omega_\alpha}\right)^2$ is called the generalized flow speed and the restoring force in the pitch DOF is given as

$$f(\alpha) = r_\alpha^2 \frac{\partial V}{\partial \alpha} = r_\alpha^2(\alpha + \delta_3\alpha^3). \tag{4}$$

For brevity, Eq. (3) is rewritten in vector form as

$$\mathbf{M}\ddot{\mathbf{x}} + \boldsymbol{\mu}\dot{\mathbf{x}} + \mathbf{K}_Q\mathbf{x} + \mathbf{F}(\mathbf{x}) = \mathbf{0}, \tag{5}$$

where

$$\mathbf{M} = \begin{bmatrix} 1 & 0.25 \\ 0.25 & 0.5 \end{bmatrix}, \quad \boldsymbol{\mu} = \begin{bmatrix} 0.1 & 0 \\ 0 & 0.1 \end{bmatrix}, \quad \mathbf{K}_Q = \begin{bmatrix} 0.2 & 0.1Q \\ 0 & 0.5 - 0.04Q \end{bmatrix},$$

$\mathbf{x} = [\xi\alpha]^{\mathrm{T}}$, and $\mathbf{F}(\mathbf{x}) = [0, k_\alpha(\mathbf{x}^{(2)})^3]^{\mathrm{T}}$ denotes the nonlinear restoring force, where $k_\alpha = r_a^2\delta_3 = 20$ is adopted to illustrate the proposed approach, $\mathbf{x}^{(2)}$ denotes the second component of vector $\mathbf{x}$, and the superscript "T" denotes the transpose.

3. Mathematical formulation

3.1. Rule of solution expression and initial guess

Firstly, introduce a new time scale τ, that

$$\tau = \omega t, \tag{6}$$

where ω denotes the angular frequency of the limit cycle, then Eq. (5) becomes

$$\omega^2\mathbf{M}\mathbf{x}'' + \omega\boldsymbol{\mu}\mathbf{x}' + \mathbf{K}_Q\mathbf{x} + \mathbf{F}(\mathbf{x}) = 0 \tag{7}$$

subject to the initial conditions

$$\mathbf{x}(0) = [h \quad a]^{\mathrm{T}}, \quad \mathbf{x}'(0) = [\beta \quad 0]^{\mathrm{T}}, \tag{8}$$

where the superscript denotes the differentiation with respect to τ.

The limit cycles of flutter system (7) are periodic motions with the angular frequency as ω, thus $\mathbf{x}$ can be expressed by a set of base functions, such as $\{\cos(k\tau), \sin(k\tau) | k = 0, 1, 2, \ldots\}$, that

$$\mathbf{x} = \sum_{k=0}^{\infty}(\mathbf{c}_k \cos k\tau + \mathbf{s}_k \sin k\tau), \tag{9}$$

where the vectors $\mathbf{c}_k$, $\mathbf{s}_k$ are the coefficients of dimension 2×1. Eq. (9) provides us with a rule, which is called the rule of solution expression. This rule is important in the frame of the homotopy analysis method, as shown later.

Let a_0, h_0, ω_0, β_0 and $\mathbf{x}_0(\tau)$ denote the initial approximations of a, h, ω, β and $\mathbf{x}(\tau)$, respectively. Considering the rule of solution expression (9) and initial conditions (8), it is obvious the initial guess of solutions can be described as

$$\mathbf{x}_0(\tau) = [h_0 \cos\tau + \beta_0 \sin\tau \quad a_0 \cos\tau]^{\mathrm{T}}. \tag{10}$$

The homotopy analysis method is based on such continuous variations $A(p)$, $H(p)$, $\Omega(p)$, $B(p)$ and $\mathbf{u}(\tau, p)$ that, as the embedding parameter p increases from 0 to 1, $\mathbf{u}(\tau, p)$ varies from the initial guess $\mathbf{x}_0(\tau)$ to the exact solutions of Eq. (7), so do $A(p)$, $H(p)$, $\Omega(p)$, $B(p)$ vary from the initial approximations a_0, h_0, ω_0, β_0 to a, h, ω, β, respectively.

3.2. Zeroth-order deformation equation

Based on the rule of solution expression described as (9), one may define the linear auxiliary operator as

$$L[(\mathbf{u}(\tau,p)] = \frac{\partial^2 \mathbf{u}(\tau,p)}{\partial \tau^2} + \mathbf{u}(\tau,p) \tag{11}$$

thus

$$L[\cos\tau] = L[\sin\tau] = 0. \tag{12}$$

Note that the rule of solution expression plays an important role in defining the linear operator. According to Eq. (7), one defines the nonlinear operator as

$$N[\mathbf{u}(\tau,p),\Omega(p)] = \Omega^2(p)\mathbf{M}\frac{\partial^2 \mathbf{u}(\tau,p)}{\partial \tau^2} + \Omega(p)\mu\frac{\partial \mathbf{u}(\tau,p)}{\partial \tau} + \mathbf{K}_Q\mathbf{u}(\tau,p) + \mathbf{F}(\mathbf{u}(\tau,p)) \tag{13}$$

and then defines the homotopy as a family of equations

$$(1-p)L[\mathbf{u}(\tau,p) - \mathbf{x}_0(\tau)] = \lambda p N[\mathbf{u}(\tau,p),\Omega(p)] \tag{14}$$

subject to the initial conditions

$$\mathbf{u}(0,p) = [\,H(p) \quad A(p)\,]^{\mathrm{T}}, \quad \left.\frac{\partial \mathbf{u}(\tau,p)}{\partial \tau}\right|_{\tau=0} = [\,B(p) \quad 0\,]^{\mathrm{T}}, \tag{15}$$

where the auxiliary parameter λ is a non-zero constant. Eqs. (14) and (15) are called the zeroth-order deformation equations.

3.3. High-order deformation equations

When $p = 0$, Eqs. (14) and (15) have the solution

$$\mathbf{u}(\tau,0) = \mathbf{x}_0(\tau), \tag{16}$$

when $p = 1$, Eqs. (14) and (15) are exactly the same as (7) and (8), so

$$\mathbf{u}(\tau,1) = \mathbf{x}(\tau), \quad A(1) = a, \quad H(1) = h, \quad \Omega(1) = \omega, \quad B(1) = \beta. \tag{17}$$

Assuming that $\mathbf{u}(\tau, p)$ and $A(p)$, $H(p)$, $\Omega(p)$, $B(p)$ have continuous derivatives with respect to p in $p \in [0, 1]$, then they can be expanded as the Maclaurin series

$$\begin{aligned} &\mathbf{u}(\tau,p) = \sum_{k=0}^{\infty}\mathbf{u}_k(\tau)p^k, \quad A(p) = \sum_{k=0}^{\infty}a_k p^k, \quad H(p) = \sum_{k=0}^{\infty}h_k p^k, \\ &\Omega(p) = \sum_{k=0}^{\infty}\omega_k p^k, \quad B(p) = \sum_{k=0}^{\infty}\beta_k p^k. \end{aligned} \tag{18}$$

As long as the parameter λ is properly chosen, all of these series are convergent at $p = 1$. Then, the mth-order solutions can be described as

$$\mathbf{x}(\tau) = \sum_{k=0}^{m}\mathbf{u}_k(\tau), \quad a = \sum_{k=0}^{m}a_k, \quad h = \sum_{k=0}^{m}h_k, \quad \omega = \sum_{k=0}^{m}\omega_k, \quad \beta = \sum_{k=0}^{m}\beta_k. \tag{19}$$

Substituting Eq. (18) into (14) and (15), equating the coefficients of p^k to be zeroes, one can obtain the kth-order deformation equation

$$L[\mathbf{u}_k(\tau) - \chi_k\mathbf{u}_{k-1}(\tau)] = \lambda\mathbf{R}_k(\tau) \tag{20}$$

subject to the initial conditions

$$\mathbf{u}_k(0) = [\,h_k \quad a_k\,]^{\mathrm{T}}, \quad \mathbf{u}_k'(0) = [\,\beta_k \quad 0\,]^{\mathrm{T}}, \tag{21}$$

where

$$\mathbf{R}_k(\tau) = \frac{1}{(k-1)!}\left.\frac{\partial^{k-1}N[\mathbf{u}(\tau,p),\Omega(p)]}{\partial p^{k-1}}\right|_{p=0} \tag{22}$$

and

$$\chi_k = \begin{cases} 0, & k = 1, \\ 1, & k \geqslant 2. \end{cases} \tag{23}$$

The zeroth-order approximation for $\mathbf{u}(\tau, p)$ is given as (10), however a_0, h_0, ω_0, β_0 are still unknown. Substituting Eqs. (10) and (16) into the right hand side of the first-order deformation equation, then one can get $\mathbf{R}_1(\tau)$. Due to the rule of solution expression and the linear operator L, the right hand side of (16) should not contain $\sin\tau$ and $\cos\tau$, because they can bring such so-called secular terms as $\tau\sin\tau$ and $\tau\cos\tau$, respectively. Letting their coefficients be zeroes, one obtains

$$\begin{aligned}\mathbf{\Gamma}_{1,c}(a_0,h_0,\omega_0,\beta_0) &= \frac{1}{\pi}\int_0^{2\pi}\mathbf{R}_1(\tau)\cos\tau\,\mathrm{d}\tau = 0,\\ \mathbf{\Gamma}_{1,s}(a_0,h_0,\omega_0,\beta_0) &= \frac{1}{\pi}\int_0^{2\pi}\mathbf{R}_1(\tau)\sin\tau\,\mathrm{d}\tau = 0.\end{aligned} \tag{24}$$

Note that Eq. (24) is in general nonlinear, which is independent of λ, thus the zeroth-order solution is independent of λ. In fact, (24) is exactly the same as that provided by the HB1 method.

Solving (24), a_0, h_0, ω_0, β_0 are then obtained, hence $\mathbf{u}_0$ is determined. Substituting them into (20) and (21) with $k = 1$, $\mathbf{u}_1(\tau)$ can then be obtained. Considering the initial conditions (21), one can see that $\mathbf{u}_1(\tau)$ is linear with respect to h_1, a_1, β_1, so is $\mathbf{u}_k$ with h_k, a_k, β_k when $k > 1$.

Assuming that a_{k-1}, h_{k-1}, ω_{k-1}, β_{k-1} and $\mathbf{u}_{k-1}(\tau)$ are obtained, then the kth-order approximations are governed by

$$\begin{aligned}\mathbf{\Gamma}_{k+1,c}(a_k,h_k,\omega_k,\beta_k) &= \frac{1}{\pi}\int_0^{2\pi}\mathbf{R}_{k+1}(\tau)\cos\tau\,\mathrm{d}\tau = 0,\\ \mathbf{\Gamma}_{k+1,s}(a_k,h_k,\omega_k,\beta_k) &= \frac{1}{\pi}\int_0^{2\pi}\mathbf{R}_{k+1}(\tau)\sin\tau\,\mathrm{d}\tau = 0.\end{aligned} \tag{25}$$

To prove that (25) is linear when $k \geqslant 1$, we consider the relationship between $\mathbf{R}_{k+1}(\tau)$ and a_k, h_k, ω_k, β_k firstly. $\mathbf{R}_{k+1}(\tau)$ can be expanded as

$$\mathbf{R}_{k+1}(\tau) = \mathbf{M}\sum_{i=0}^{k}\sum_{j=i}^{k}\omega_i\omega_{j-i}\mathbf{u}''_{k-j} + \boldsymbol{\mu}\sum_{i=0}^{k}\omega_i\mathbf{u}'_{k-i} + \mathbf{K}_Q\mathbf{u}_k + \begin{bmatrix}0 & k_\alpha\sum_{i=0}^{k}\sum_{j=i}^{k}\mathbf{u}_i^{(2)}\mathbf{u}_{j-i}^{(2)}\mathbf{u}_{k-j}^{(2)}\end{bmatrix}^{\mathrm{T}} = N_1\mathbf{u}_k + N_2\omega_k, \tag{26}$$

where $\mathbf{u}_i^{(2)}$ denotes the second component of $\mathbf{u}_i$, and N_1, N_2 are functions of $a_0, h_0, \omega_0, \omega_{k-1}, \ldots, a_{k-1}, h_{k-1}, \omega_{k-1}, \beta_{k-1}$ and τ, but independent of $a_k, h_k, \omega_k, \beta_k$. As we know, $\mathbf{u}_k(\tau)$ is linear with respect to h_k, a_k, β_k, thus $\mathbf{R}_{k+1}(\tau)$ is linear with respect to $a_k, h_k, \omega_k, \beta_k$. Accordingly, Eq. (25) is linear when $k \geqslant 1$, which implies as long as the auxiliary parameter is properly chosen, we can obtain the solutions to any desired accuracy rather easily.

4. Results and discussion

First of all, the following analysis is limited for generalized flow speed lower than the static divergence speed $Q_d = 12.5$, i.e., $Q \leqslant Q_d$, because the static divergence has to be avoided in aircraft engineering [25].

Using the Hopf bifurcation theory, a supercritical Hopf bifurcation of system (5) can be found as $Q_f = 4.08$. Note that in the proposed approach, this bifurcation point can be exactly found using Eq. (24). Thus, the bifurcation charts in the region of $[Q_f, Q_d]$ are plotted in Fig. 2, which shows the comparisons of the results obtained by the proposed method and the HB1 method with the numerical solutions. From it we can see, the 30th-order solutions by the presented approach are much more accurate than the HB1 results, especially for relatively larger flow speed.

Due to the fact that the higher approximations of ω_k, a_k, h_k and β_k are governed by linear algebraic equations when $k \geqslant 1$, it is quite easy to compute them to very high order. The solutions to the 150th-order are shown in Table 1. To give more insight into the convergence of series (18), they are obtained to the 10th, 50th, 100th and 150th-order, respectively. Note that it is proved by Liao [11] that as long as the series given by HAM is convergent, it must converge to one solution of the problem under consideration. From Table 1, we can see that the 150th-order solutions converge to the solutions correct to many decimal places. Unfortunately, it is not easy to calculate the amplitudes and the frequencies accurately enough to validate the convergent solutions provided by the presented method. Alternatively, we check whether the solutions given by the presented method satisfy Eq. (5). As a result, the high accuracy can be observed from Fig. 3, which shows the residuals on one period, where the residuals are defined as

$$\mathbf{Re}(\mathbf{x}) = [\mathbf{Re}_1(\mathbf{x}), \mathbf{Re}_2(\mathbf{x})]^{\mathrm{T}} = \mathbf{M}\ddot{\mathbf{x}} + \boldsymbol{\mu}\dot{\mathbf{x}} + \mathbf{K}_Q\mathbf{x} + \mathbf{F}(\mathbf{x}),$$

where $\mathbf{x}$ is obtained by the presented method.

The HAM is implemented under the assumption the Maclaurin series (18) of the auxiliary parameter p are all convergent at $p = 1$. That means the convergence of series (18) has a quite relevant place in the frame of the proposed method. Note that the convergence of series (18) is dependent on the auxiliary parameter λ. Fig. 4 shows the difference between the 30th-order frequency solutions and the numerical results versus varying λ and $Q = 10$. We can see that in the convergent region, say $h \in (-3.50)$ or so: (1) higher order solutions are more accurate; (2) solutions obtained with smaller λ are more accurate. These two properties can also be reflected in Table 1. For example, for the case of $Q = 6$, the solutions obtained with $\lambda = -1$ to the 10, 50 and 100th-order are correct to 2, 4 and 6 decimal places, respectively, while the solutions obtained with $\lambda = -3$ to the 10, 50 and 100th-order converge to 4, 11 and 13 decimal places, respectively.

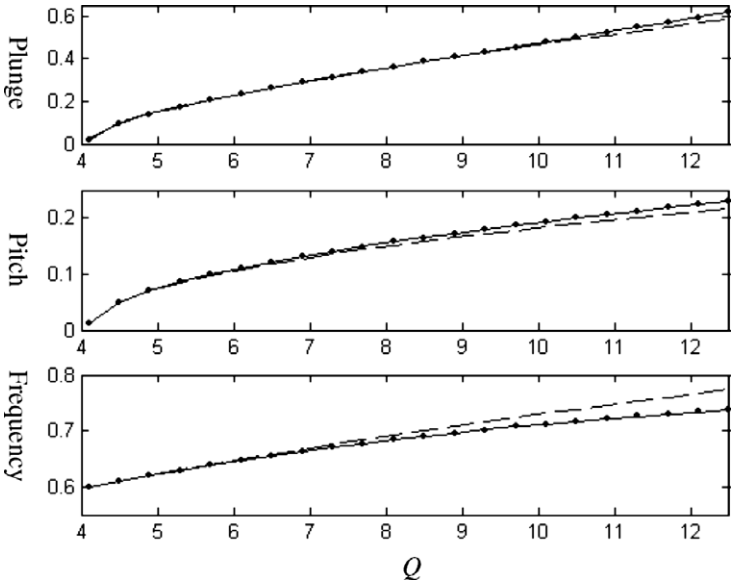

Fig. 2. Comparisons of the amplitudes and frequencies of the limit cycle flutter. Dot lines for the 30th-order solutions with $\lambda = -1$, dashed lines for the HB1 solutions, solid lines for numerical solutions.

Table 1
The solutions for frequencies and amplitudes in the pitch DOF obtained by the proposed method

λ	m	$Q = 6$		$Q = 10$	
		Pitch (a)	Frequency (ω)	Pitch (a)	Frequency (ω)
−1	10	0.10891045428506	0.63643839743767	0.19026365161099	0.71949827165672
	50	0.10787145527603	0.64459377993858	0.19175610837202	0.71017162760398
	100	0.10785737827058	0.64466900688545	0.19177097258524	0.71009098244943
	150	0.10785723873990	0.64466966987558	0.19177111333200	0.71009031348370
−3	10	0.10784955759690	0.64473108073014	0.19167513983327	0.71069481254337
	50	0.10785723874195	0.64466966986659	0.19177111438572	0.71009030753800
	100	0.10785723874211	0.64466966986595	0.19177111510464	0.71009030550733
	150	0.10785723874211	0.64466966986595	0.19177111510464	0.71009030550733

Since series (18) are obtained to very high order, we apply the root criterion for the convergence of series to determine the convergence radius roughly. The convergence radius of series expansion for frequency can be obtained approximately in Fig. 5 or Fig. 6. Interestingly, it is shown in Fig. 5 the convergence radius is larger than 1 and increases as λ in the convergent region decreases. However once λ is beyond the convergent region, e.g., when $\lambda = -4$, the radius becomes smaller than 1, which means series (18) do not converge at $p = 1$. From Fig. 6, we can see when Q and λ are given, the series expansions for $A(p)$, $H(p)$, $B(p)$ and $\Omega(p)$ have the same convergence radius. Note that the larger the convergence radius of series (18) is, the faster series (19) converges. That is why the solutions obtained with $\lambda = -3$ converge faster than those obtained with $\lambda = -1$, as shown in Table 1.

For the choice of the auxiliary parameter, one would think about two issues, i.e., whether the series converge and the convergent rate. According to the analysis above, on the one hand, we want to choose the auxiliary parameter as small as possible to improve the convergent rate. On the other hand, we are prone to choose an improper value, leading to that the series given by the proposed method don't converge at $p = 1$.

Now we turn to talk about the relationship between the convergence of series (18) and the coefficient of the cubic nonlinearity, i.e., k_α. Interestingly, it is found that ω_i is independent of k_α, while a_i,β_i and h_i is in inverse proportion to $\sqrt{k_\alpha}$. Thus, the convergence is independent of k_α and the proposed method can work for weakly as well as strongly nonlinear problems. Accordingly, it is proved that the frequency of the limit cycle oscillations of flutter system (5) is independent of k_α, which is claimed by Cai et al. [31] without proof. And, it is also found the amplitudes of the limit cycle flutter are in inverse proportion to $\sqrt{k_\alpha}$.

Let $C_\alpha(k_\alpha)$, $C_\xi(k_\alpha)$ be the amplitudes of the limit cycle of the system (5) in the pitch and plunge DOFs with respect to k_α, respectively. Then the amplitudes in the pitch and plunge DOFs can be given as functions of k_α as $C_\alpha(k_\alpha) = C_\alpha(1)/\sqrt{k_\alpha}$, and

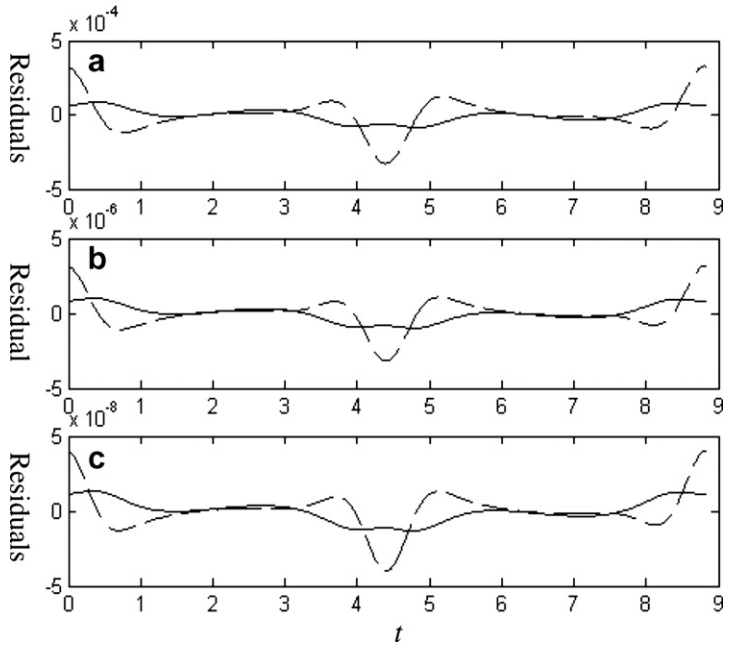

Fig. 3. Residuals of Eq. (5) with the HAM solutions on one period with $Q = 10$ and $\lambda = -1$, where (a) for $m = 50$; (b) for $m = 100$; (c) for $m = 150$. Solid lines denote $\mathbf{Re}_1(\boldsymbol{x})$, dashed lines denote $\mathbf{Re}_2(\boldsymbol{x})$.

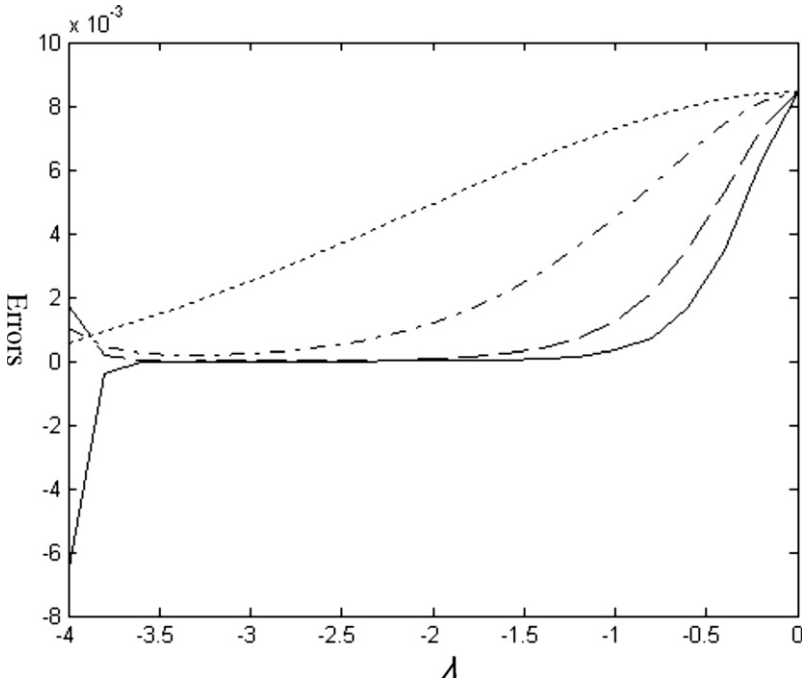

Fig. 4. Errors of frequencies of limit cycles versus with varying λ and $Q = 10$, where solid line denotes the 30th-order solutions, dashed line for the 20th-order solutions, dash-dot line for the 10th-order solutions and dot line for the 5th-order solutions.

$C_{\xi}(k_{\alpha}) = C_{\xi}(1)/\sqrt{k_{\alpha}}$, respectively. Fig. 7 shows the curves of the amplitudes versus k_{α}, where $C_{\alpha}(1)$ and $C_{\xi}(1)$ are given by the 20th-order solution by the presented method. We can see that the solutions obtained by the proposed method are in excellent agreement with the numerical ones.

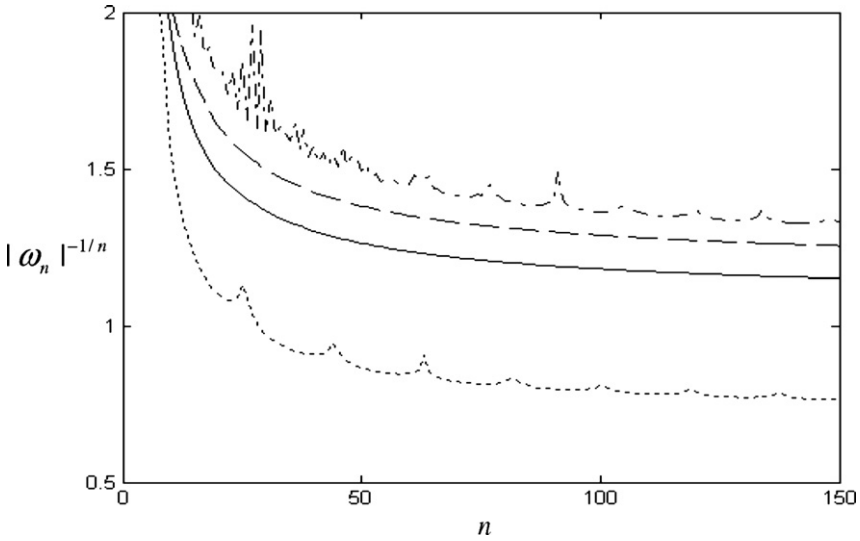

Fig. 5. Root criterion for the radius of the convergence of the series expansion for frequency with $Q = 10$, solid line for $\lambda = -1$, dashed line for $\lambda = -2$, dash-dot line for $\lambda = -3$ and dot line for $\lambda = -4$.

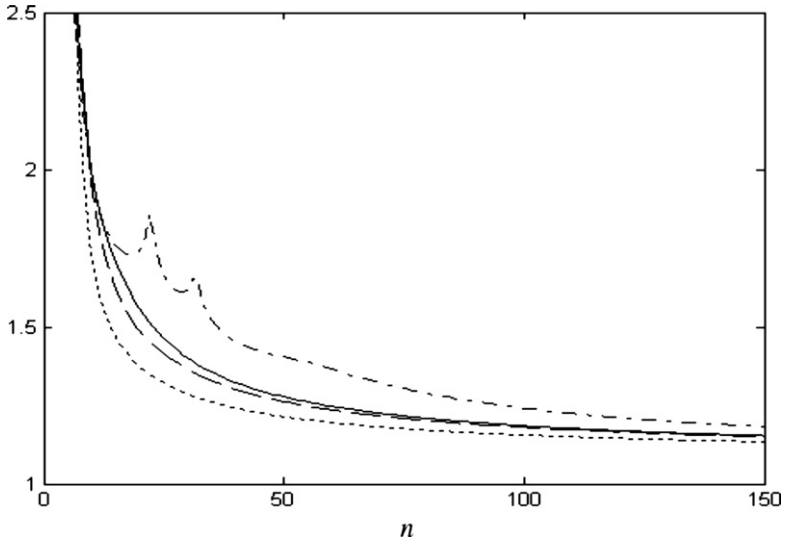

Fig. 6. Root criterion for the radius of the convergence of the series (14) with $\lambda = -1$, $Q = 10$. Real line for $|a_n|^{-1/n}$, dashed line for $|h_n|^{-1/n}$, dash-dot line for $|\beta_n|^{-1/n}$, dot line for $|\omega_n|^{-1/n}$.

5. Conclusions

The homotopy analysis method is firstly implemented in nonlinear flutter systems. The frequencies and amplitudes of the limit cycles are obtained with very high accuracy. In fact, the solutions with any desired degree of accuracy can be easily obtained by the proposed approach. A major finding of this study is the dependence of the amplitudes and frequency of limit cycle flutter on the nonlinear coefficient, which seems difficult to be found by the existing analytical methods.

The zeroth-order solution is essentially the HB1 result, so the proposed method can also be treated as an improvement of HB1 method. Thus, as long as the solutions can be found by HB1 method, the accuracy can be improved to any desired degree by the presented method. And, it can work for weakly and strongly nonlinear aeroelastic systems, which implies we would expect the proposed method to be applicable in more nonlinear aeroelastic systems, especially those with strong nonlinearities.

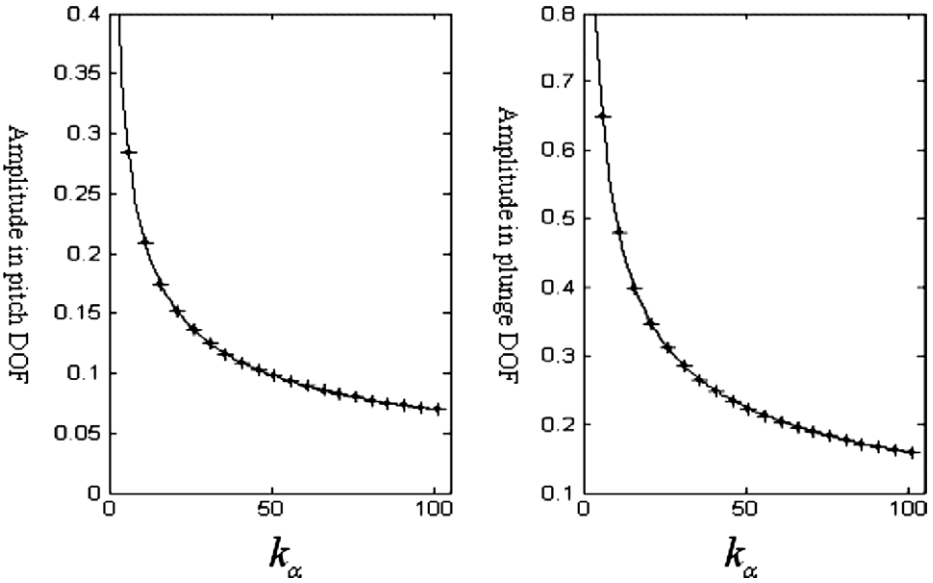

Fig. 7. Curves of the amplitudes of the limit cycle of system (5) versus k_α with $Q = 8$. Real lines are given by $C_\alpha(k_\alpha)$ or $C_\xi(k_\alpha)$, dots denote 20th-order solutions with $\lambda = -3$ and "+" denotes numerical solutions.

Acknowledgements

This work is supported by the National Natural Science Foundation of China (10772202), Doctoral Program Foundation of Ministry of Education of China (20050558032), Guangdong Province Natural Science Foundation (07003680, 05003295).

References

[1] E.L. Allgower, K. Georg, Numerical Continuation Methods, Springer-Verlag, Berlin, 1990.
[2] S.N. Chow, J. Mallet-Paret, J.A. Yorke, Finding zeroes of maps: homotopy methods that are constructive with probability one, Math. Comput. 32 (1978) 887–899.
[3] L.T. Watson, Globally convergent homotopy algorithms for nonlinear systems of equations, Nonlinear Dyn. 1 (1990) 143–191.
[4] V. Arun, C.F. Reinholtz, L.T. Waston, Application of new homotopy continuation techniques to variable geometry trusses, J. Mech. Design 114 (1992) 422–427.
[5] L.T. Watson, Theory of globally convergent probability-one homotopies for nonlinear programming, SIAM J. Optim. 11 (3) (2000) 180–761.
[6] L.T. Watson, Probability-one homotopies in computational science, J. Comput. Appl. Math. 140 (2002) 785–807.
[7] S.J. Liao, A second-order approximate analytical solution of a simple pendulum by the process analysis method, J. Appl. Mech. 59 (1992) 970–975.
[8] S.J. Liao, An approximate solution technique not depending on small parameters: a special example, Int. J. Non-linear Mech. 30 (1995) 371–380.
[9] S.J. Liao, A kind of approximate solution technique which does not depend upon small parameters-II: an application in fluid mechanics, Int. J. Non-linear Mech. 32 (5) (1997) 815–822.
[10] S.J. Liao, On the homotopy analysis method for nonlinear problems, Appl. Math. Comput. 147 (2004) 499–513.
[11] S.J. Liao, An explicit, totally analytic approximate solution for Blasius' viscous flow problems, Int. J. Non-linear Mech. 34 (1999) 759–778.
[12] S.J. Liao, An analytic approximate approach for free oscillations of self-excited system, Int. J. Non-linear Mech. 39 (2004) 271–280.
[13] S.J. Liao, An explicit analytic solution to the Thomas–Fermi equation, Appl. Math. Comput. 144 (2003) 495–506.
[14] T. Hayat, M. Khan, S. Asghar, Magnetohydrodynamic flow of an Oldroyd 6-constant fluid, Appl. Math. Comput. 155 (2004) 417–425.
[15] S. Asghar, M.M. Gulzar, T. Hayat, Rotating flow of a third grade fluid by homotopy analysis method, Appl. Math. Comput. 165 (2005) 213–221.
[16] S.C. Li, S.J. Liao, An analytic approach to solve multiple solutions of a strongly nonlinear problem, Appl. Math. Comput. 169 (2005) 854–865.
[17] J.H. He, Homotopy perturbation technique, Comput. Meth. Appl. Mech. Eng. 178 (3/4) (1999) 257–262.
[18] J.H. He, A coupling method of homotopy technique and perturbation technique for nonlinear problems, Int. J. Nonlinear Mech. 35 (1) (2000) 37–43.
[19] J.H. He, Homotopy perturbation method: a new nonlinear analytical technique, Appl. Math. Comput. 135 (2003) 73–79.
[20] J.H. He, The homotopy perturbation method for nonlinear oscillators with discontinuities, Appl. Math. Comput. 151 (2004) 287–292.
[21] J.H. He, Some asymptotic methods for strongly nonlinear equations, Int. J. Modern Phys. B 20 (10) (2006) 1141–1199.
[22] B.H.K. Lee, S.J. Price, Y.S. Wong, Nonlinear aeroelastic analysis of airfoils: bifurcation and chaos, Prog. Aerosp. Sci. 35 (1999) 205–344.
[23] S.F. Shen, An approximate analysis of nonlinear flutter problems, J. Aerosp. Sci. 26 (1959) 25–32.
[24] S.F. Price, H. Alighanbari, B.H.K. Lee, The aeroelastic response of a two-dimensional airfoil with bilinear and cubic structural nonlinearities, J. Fluids Struct. 9 (1995) 175–193.
[25] J.K. Liu, L.C. Zhao, Bifurcation analysis of airfoils in incompressible flow, J. Sound Vib. 154 (1) (1991) 117–124.
[26] P. Shahrzad, M. Mahzoon, Limit cycle flutter of airfoils in steady and unsteady flows, J. Sound Vib. 256 (2) (2002) 213–225.
[27] Y.R. Yang, KBM method of analyzing limit cycle flutter of a wing with an external store and comparison with wind tunnel test, J. Sound Vib. 187 (2) (1995) 271–280.
[28] L.P. Liu, E.H. Dowell, Harmonic balance approach for an airfoil with a Freeplay control surface, AIAA J. 43 (4) (2005) 802–815.
[29] L.P. Liu, J.P. Thomas, E.H. Dowell, P.J. Attar, K.C. Hall, A comparison of classical and high dimensional harmonic balance approaches for a Duffing oscillator, J. Comput. Phys. 215 (1) (2006) 298–320.
[30] L.P. Liu, E.H. Dowell, The secondary bifurcation of an aeroelastic airfoil motion: effect of high harmonics, Nonlinear Dyn. 37 (2004) 31–49.
[31] M. Cai, J.K. Liu, J. Li, Incremental harmonic balance method for airfoil flutter with multiple strong nonlinearities, Appl. Math. Mech. 27 (7) (2006) 953–958.

[32] B.H.K. Lee, L.Y. Jiang, Y.S. Wong, Flutter of an airfoil with cubic restoring force, J. Fluids Struct. 13 (1999) 75–101.
[33] B.D. Coller, P.A. Chamara, Structural non-linearities and the nature of the classic flutter instability, J. Sound Vib. 277 (2004) 711–739.
[34] K.C. Hall, J.P. Thomas, E.H. Dowell, Proper orthogonal decomposition technique for transonic unsteady aerodynamic flows, AIAA J. 38 (2000) 1853–1862.
[35] J.P. Thomas, E.H. Dowell, K.C. Hall, Modeling viscous transonic limit cycle oscillation behavior using a harmonic balance approach, J. Aircraft. 41 (6) (2004) 1266–1274.